Transactions of the VŠB – Technical University of Ostrava, Mechanical Series
No. 3, 2010, vol. LVI
article No. 1821

David LÁVIČKA *

TEMPERATURE FIELD PROGRESSION IN ANNULAR TUBE AROUND HEATED ROD IN RESPECT TO THE MASS FLOW OF COOLANT

PRŮBĚH TEPLOTNÍHO POLE V MEZIKRUHOVÉM PRŮTOČNÉM KANÁLE OKOLO VYHŘÍVANÉ TYČE V ZÁVISLOSTI NA PRŮTOČNÉM MNOŽSTVÍ CHLADÍCÍ KAPALINY

Abstract

The paper looks into liquid flow simulation in the annular tube around the heated rod. The numerical simulation serves primarily the purpose of describing the temperature field in the annular tube that represents a simplified model of a nuclear reactor fuel rod. The fuel rod model uses several configurations of spacers which affect the flow of coolant - water - in the annular flow channel. For selected variants of spacers, temperature fields have been mutually compared in respect to various mass flow characteristics of the coolant.

Abstrakt

Příspěvek se věnuje simulaci proudění kapaliny v mezikruhovém průtočném kanále okolo vyhřívané tyče. Numerická simulace slouží hlavně k popisu teplotního pole v průtočném kanále představující zjednodušený model palivové tyče jaderného reaktoru. Na modelu palivového proutku jsou použity různé konfigurace distančních mřížek ovlivňující proudění chladicího média, vody, v průtočném mezikruhovém kanále. Pro vybrané tvary distančních mřížek je provedeno vzájemné srovnání teplotního pole v závislosti na různém průtočném množství chladící kapaliny.

1 INTRODUCTION

Numerical simulation of the velocity and temperature flow field in the annular tube is based on the experimental apparatus build at the Department of Power System Engineering at University of West Bohemia in Pilsen. The special experimental apparatus is primarily used for research in the domain of heat transfer at models of nuclear reactor fuel rods. The main topic is study of generation of steam (gas) bubbles that affect flow and heat transfer from the heated stainless-steel pipe into the coolant. The quantity of heat transferred is affected by various shapes of spacers which serve several important purposes. Their first role is central alignment of the stainless-steel tube (representing the fuel rod at the nuclear power station) inside a glass tube. Another purpose of the spacer is generation of vortex. The intensity of vortex affects heat transfer between the heated stainless-steel tube and the flowing coolant. Here, the coolant is water with specified boundary conditions.

This paper focuses on the comparison of the velocity and temperature flow fields in settled condition in relation to the shape of the spacer and to the quantity of water mass flow. Selected spacer shapes were inserted into the annular tube model of the fuel rod; these spacers were analyzed and compared one to another for mutual assessment of the observed properties of the spacers being used.

* Ing., Ph.D.; University of West Bohemia, Department of Power System Engineering (KKE), Univerzitni 8, 306 14 Plzen, phone: +420 377 634 712, email: dlavicka@ntc.zcu.cz

2 COMPUTATIONAL MODEL

The computational geometry is based on the dimensions of a real fuel rod in the nuclear reactor; the rod is also used at the experimental apparatus for study of two-phase flow. Description of the computational model with location of the spacer and basic dimensions of the annular channel with the stainless-steel tube is provided in Figure 1. The GAMBIT software was used to prepare 3 computational meshes for 3 different spacer shapes. Individual spacer shapes are also shown in Figure 1.

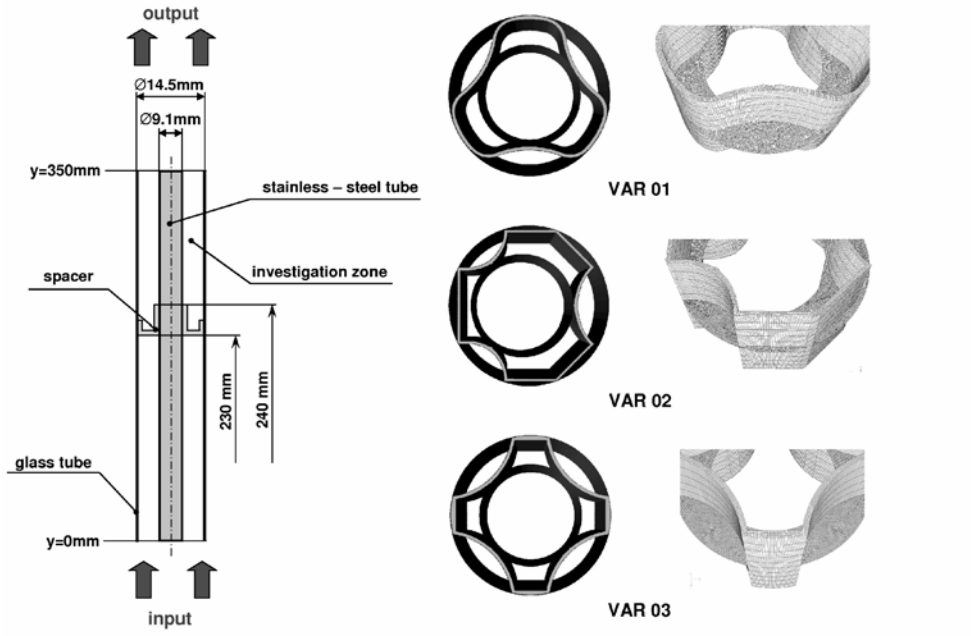

Fig. 1 Fuel rod model and shapes of selected individual spacers in the annular tube

The base of the model is an area in the shape of the spacer, projected perpendicularly onto the inlet plane. In this plane, the surface mesh was modeled with quad elements. The number of surface elements in the plane ranges around 25,000. Figure 1 shows an example of the spacer surface mesh.

The volumetric mesh was obtained by application of the "cooper" function (similar to "sweep") in the GAMBIT software. The vertical number of elements is not distributed uniformly, with higher cell density in the spacer area and its immediate vicinity. The volumetric mesh contains approximately 1.3 million cells.

3 NUMERICAL SIMULATION

The boundary conditions for numerical simulation are described in Figure 1. The lower part of the flow channel holds a defined boundary input condition of "mass-flow inlet" to specify the flow rate. Flow rate was set in four different values, in the range from 0.0005 kg/s to 0.0014 kg/s. A "pressure-outlet" boundary condition was set at the outlet. The numerical simulation was conducted in the FLUENT CFD software. The flowing medium is water; its properties have been set to resemble the true conditions inside the nuclear reactor.

The numerical simulation was divided into a series of several steps to improve the stability and accuracy of the calculation. The calculation was run as isothermal flow with the "RSM – Low-Reynolds Stress-Omega" turbulence model at the first order of accuracy. After the residual values have settled in the calculation, temperature of the stainless-steel tube and spacer was set at 370 K (approximately 97 °C). Parameters of the water were not input for atmospheric pressure; therefore, water at this temperature is not near the boiling point. The calculation then continued in the

non-stationary mode at the second order of accuracy by 300 time steps with a period of 0.02 s. The results for comparison of the examined properties of the spacers were obtained from the non-stationary mode with time-mean (average) values at the second order of accuracy from 200 time steps with identical period length.

4 RESULTS

A summary of important characteristic data and results is provided in Table 1. An important value is the pressure loss caused by the spacer; this was calculated by subtraction of the pressure before and after the spacer.

Tab. 1 Characteristic data and results of the spacers at various flow levels

spacer	**VAR 01**				**VAR 02**				**VAR 03**			
mass flow rate Q_m [kg/s]	0,0005	0,0007	0,0010	0,0014	0,0005	0,0007	0,0010	0,0014	0,0005	0,0007	0,0010	0,0014
pressure p [Pa]	0,082	0,126	0,197	0,310	0,102	0,156	0,247	0,391	0,110	0,148	0,245	0,357
velocity w_y^* [m/s]	0,0055	0,0076	0,0109	0,0153	0,0056	0,0078	0,0112	0,0156	0,0061	0,0077	0,0116	0,0154
temperature at the annular tube T^* [K]	347,7	346,5	345,3	344,3	352,7	351,4	350,0	348,5	347,7	346,9	345,6	344,7
coefficient hydraulic resistance ξ^* [1]	62	48	33	25	67	49	35	26	60	49	33	25
Re number [1]	99	138	198	277	99	138	198	277	99	138	198	277

The following result is the mean average temperature on the surface inside the annular tube in the spacer area. In Table 1, the indicated values were applied to calculate the local loss coefficient ξ [1] for individual spacer types. The value of the local loss coefficient was calculated using the formula (1) and the Reynolds number at the channel inlet as per formula (2).

$$p_{\xi} = \xi \frac{\rho \cdot w^2}{2} \tag{1}$$

$$\mathrm{Re} = \frac{\rho \cdot w \cdot D_{\mathrm{H}}}{\mu} \tag{2}$$

The hydraulic diameter (3), D_H, is used to calculate the dimensionless Reynolds Number to determine if a flow is turbulent or laminar.

$$D_H = \frac{4A}{P} = \frac{4\pi\left(\frac{D^2 - d^2}{4}\right)}{\pi(D + d)} = D - d \tag{3}$$

where A is the cross sectional area and P is the wetted perimeter of the cross-section. In this case used simplified annular tube, which is described on formula (3). The final formula (3) describe difference diameters, where D is inside radius of the outside tube and d is outside radius of the inside tube.

The indicated results imply that the lowest resistance as seen in the spacer marked as VAR 01 and on the contrary, the spacer with the highest resistance is VAR 02. The latter also indicates highest

level of coolant heating at the section of the annular tube; the temperature at channel section is by 5 K higher than in the other variants.

The charts of Figure 3 illustrate vertical progression of temperature at the annular tube. Two measurement points were selected to provide comparison of individual spacers. Measurement point 1 is located in a "warmer spot". This point is on one side surrounded by the heated stainless-steel tube and the spacer. Point 2 was selected in a "colder spot"; one side is surrounded by the glass tube and the other by the spacer. Both points lie in an identical circle which passes approximately through the center of these delimited areas. Position of these points is shown in the legend at Figure 2; they are also indicated in Figures 3 and 4.

In respect to both measurement points, notable difference may be seen between the temperatures of the individual areas. In comparison to Point 2, temperature in Point 1 is higher by approximately 25 K. This fact is caused by higher cooling rate of the coolant through the glass tube into the ambient area around the fuel rod model.

It is more than worthwhile to look at the behavior of the temperature field in the spacer area: this position is in the channel indicated by grey dotted line at x-coordinates of 0.230 mm and 0.240 mm. In this location, the coolant is heated by flow turbulence behind the inserted spacer.

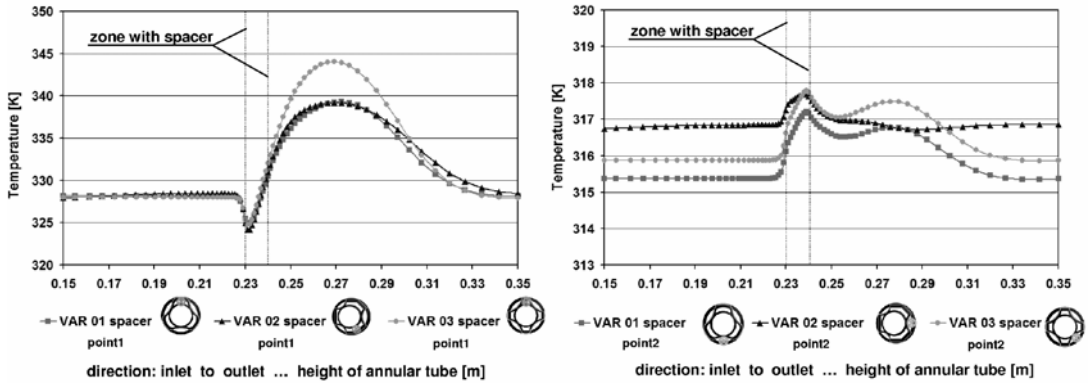

Fig. 2 Temperature progression along the channel in the two measurement points for different spacer geometries

The charts shown in Figures 3 and 4 depict the vertical progression of temperature in the annular tube for various flow rates for variants VAR 01 and VAR 03. The temperature values of the spacer and stainless-steel tube were again set at 370 K. In all three variants for the individual flow rates, identically defined points 1 and 2 were monitored.

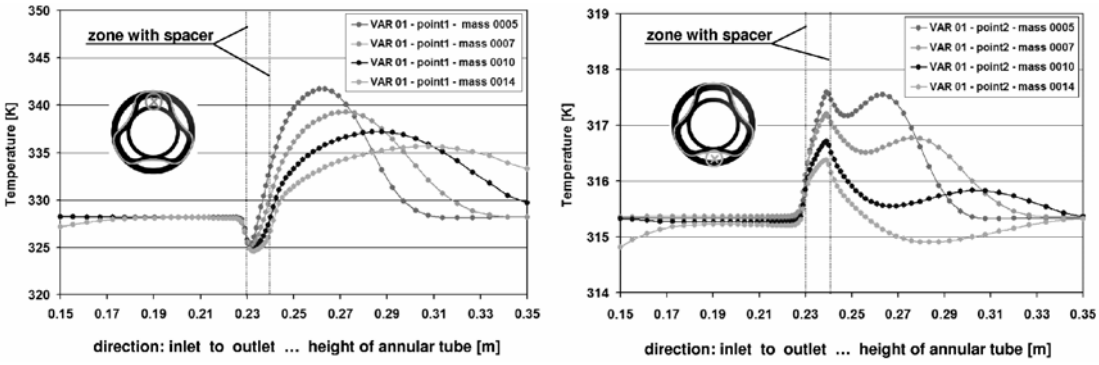

Fig. 3 Temperature progression along the channel in the two measurement points for VAR 01

Only variants VAR 01 and VAR 03 were selected for comparison of temperature progression because the VAR 02 variant has shown progression nearly identical to that of VAR 01. The VAR 03 variant in Point 1 shows higher coolant temperature behind the spacer in all the flow rates tested. Another phenomenon studied is cooling of the coolant almost to the initial level. As the flow rate gradually increases, the length of cooling disproportionally extends; with some of the flow rates, this occurs beyond the chart area shown.

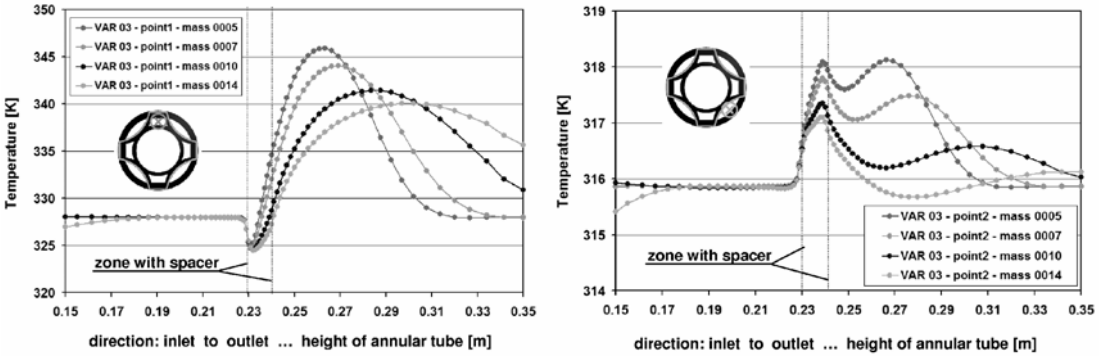

Fig. 4 Temperature progression along the channel in the two measurement points for VAR 03

It is also with Point 2 that the VAR 03 variant shows higher increment of temperature; however, this occurs in the spacer area. Flow rates of 0.0005 kg/s and 0.0007 kg/s show mild temperature drop only to experience notable reheating of the coolant. Subsequently, the coolant cools fully, almost to the initial temperature. On the other hand, in flow rates of 0.0010 kg/s and 0.0014 kg/s, similarly to the flow rates mentioned above, heating occurs in the spacer area but then the coolant cools down rapidly and later heats up only a little. All curves meet in Point 2 at the same final temperature in the distance of 0.35 m.

The contours of the velocity and temperature fields are also highly interesting; they were assessed at planes 0.231, 0.242, and 0.250 mm in Figure 5. The spacer inserted into the annular tube is found between 0.230 and 0.240 mm. These contours indicate that the biggest differences in the coolant flow velocity are found in the VAR 02 variant. The temperature field in Figure 5, variant VAR 02, indicates an area of distinctively higher temperature at the right side of the spacer. This situation may lead to undesirable overheating of the coolant in the vertical annular tube behind the installed spacer.

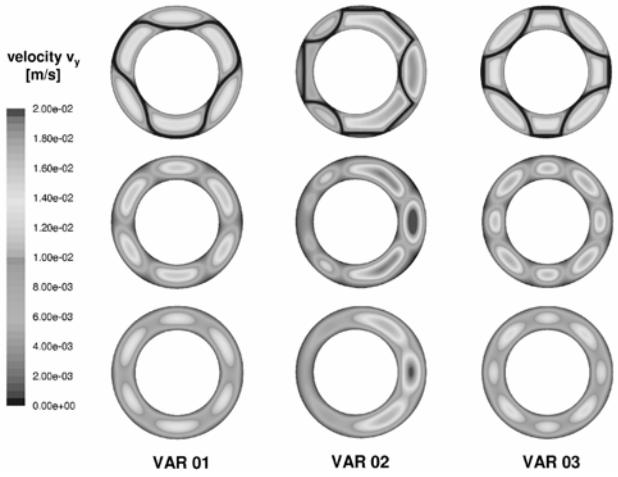

Fig. 5 Flow fields of individual spacer geometries VAR 01, VAR 02, VAR 03

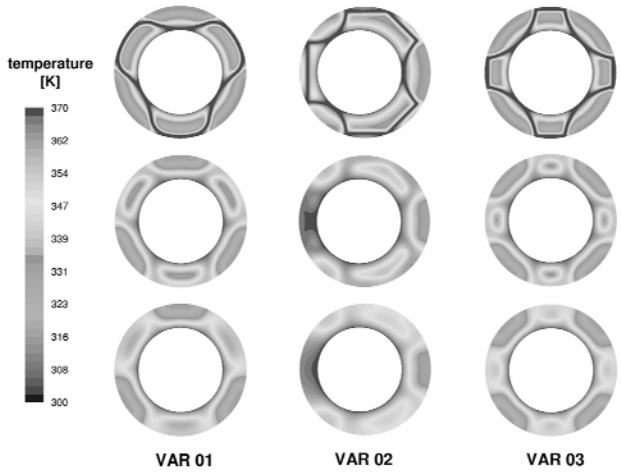

Fig. 6 Temperature fields of individual spacer geometries VAR 01, VAR 02, VAR 03

5 CONCLUSION

This experience may serve as a source of information for optimization of spacer shape; this will lead to better distribution of the temperature profile at the annular tube and to improved heat transfer between the fuel rod and coolant. These numerical simulations indicate that another major influence is the coolant flow rate. In the second half of 2010, spacers of these shapes will be produced; experimental measurements for comparison the results with the numerical simulation will follow.

6 ACKNOWLEDGEMENTS

This work was supported by the Czech Grant Agency project No. 101/09/P056 and in specific research.

REFERENCES

[1] LÁVIČKA D.: Od jaderného reaktoru k experimentálnímu modelu chlazení palivového proutku. *Modelování a měření v energetice - Tepelné cykly, jaderně energetická zařízení,* Hrad Nečtiny, Česká republika, květen 2010. ISBN 978-80-02-02239-8.

[2] LÁVIČKA, D.: Popis řešení numerických simulací v mezikruhovém průtočném kanále okolo nerezové trubky. *Stretnutie katedier mechaniky tekutin a termomechaniky,* Jasna, Demanovska dolina, Slovensko, červen 2009. ISSN 1335-2938.

[3] LÁVIČKA D.: Rychlostní a teplotní proudové pole v mezikruhovém průtočném kanále okolo vyhřívané tyče. *XVII. Aplikácia experimentálnych a numerických metód v mechanike tekutín a v energetike,* Bojnice, Slovenská republika, duben 2010. ISBN 978-80-554-0189-8.

[4] HEŘMANSKÝ B.,: *Techmomechanika reaktorů*, ČVUT, Praha, 1983.

[5] INCOPERA; DEWITT; BERGMAN; LAVINE: *Fundamentals of Heat and Mass Transfer*. 6th edition, October 30, 2006, USA. ISBN 978-0-471-45728-2.

[6] KOLEV N.I.: *Multiphase Flow Dynamics – 4 Nuclear Thermal Hydraulics*. 1ST edition, Springer. ISBN 978-3-540-92917-8.